



CHORUS

This is the accepted manuscript made available via CHORUS. The article has been published as:

Coupled electron-heat transport in nonuniform thin film semiconductor structures

V. G. Karpov

Phys. Rev. B **86**, 165317 — Published 15 October 2012

DOI: [10.1103/PhysRevB.86.165317](https://doi.org/10.1103/PhysRevB.86.165317)

Coupled electron–heat transport in nonuniform thin film semiconductor structures

V. G. Karpov

Department of Physics and Astronomy, University of Toledo, Toledo, OH 43606, USA

A theory of transverse electron transport coupled with heat transfer in semiconductor thin films is developed conceptually modeling structures of modern electronics. The transverse currents generate Joule heat with positive feedback through thermally activated conductivity. This can lead to instability known as thermal runaway, or hot spot, or reversible thermal breakdown. A theory here is based on the optimum fluctuation method modified to describe saddle stationary points determining the rate of such instabilities and conditions under which they evolve. Depending on the material and system parameters, the instabilities appear in a manner of phase transitions, similar to either nucleation or spinodal decomposition.

PACS numbers: 72.60.+g, 72.80.Ng, 64.60.Q-, 73.50.Fq

I. INTRODUCTION

Various treatments of electronic transport in disordered systems typically concentrate on systems at a given fixed temperature. However, observations (see references below) often point at the coupled electron-heat transport where local fluctuations in electric current generate temperature fluctuations. When the latter have positive feedback, as e. g. in the case of thermally activated conductivity, an instability arises leading to the current filamentation. ‘Weak spots’ corresponding to suitable disorder configurations promote such instabilities. While this mechanism has long been known qualitatively,¹ its quantitative understanding remains insufficient leaving open questions about the role of material and structure parameters, and effects of static vs. thermodynamic fluctuations.

This work attempts a theory of coupled electron-heat transport concentrating on a rather representative case of transverse conduction through thin-film structures. A model structure consists of an active (heat generating) conducting layer between two identical electrically inactive thermally insulating layers representing encapsulation always found with electronic devices. The top half of the structure is depicted in Fig. 1; the second half is symmetric with respect to the bottom line of the diagram. The active layer can be a single or multi-layered semiconductor sandwiched between thin metal electrodes. The electric potential along each of the electrodes is constant; the potential difference V between them is maintained by an external power source. The boundary conditions are that the temperature T is fixed, $T = T_0$ at the top and the bottom (not shown in in Fig. 1) surfaces of the structure where fluctuations are suppressed by thermal exchange with ambient.

The disorder is introduced through the activated transversal electric conduction with random Gaussian activation barriers varying in the lateral (along the film) directions. The role of insulating layers is that they affect the temperature distribution and make the entire model more realistic. For simplicity, we assume one of them totally insulating while another one having a finite thermal

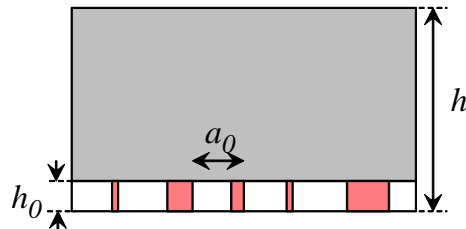


FIG. 1: Sketch of the top half of the system of total thickness $2h$ with a nonuniform power generation in the active layer of thickness $2h_0$ (reddish columns). The top thermally insulating layer is shown in gray.

conductivity. Also, for simplicity, thermal conductivities and specific heats of the active and insulating layers are assumed the same.

The analysis below is aimed at finding the probability of local temperature fluctuations and their radii associated with locally increased current density vs. the system dimensions, material parameters, and ambient temperature. It is based on the premise of localized rare lateral fluctuations that do not overlap. These localized entities are similar to other types of localized states in disordered systems, for which theoretical description known as the optimum fluctuation method (OFM) has been developed long ago. OFM was originally created to describe electronic states in band tails of disordered semiconductors;^{2–6} it was applied later to localized sound excitations in glasses,⁷ resonance electronic states in disordered metals,^{8,9} fluctuation tail states in magnetic semiconductors,¹⁰ random lasing in disordered dielectric films,¹¹ local fluctuations in thermal expansion of glasses,¹² and nucleation in disordered media.¹³

The essence of OFM is in the optimization of configurational probability of fluctuations under the additional condition that the dynamical characteristic of a fluctuation satisfies the appropriate differential equation (Schrödinger equation for electronic state, elastic wave equation for sound excitations, electromagnetic wave equation for optic modes, etc.). This is achieved through the variational approach, in which the dynamical charac-

teristic is kept fixed (yet arbitrary) in the course of optimization of the configurational probability, after which it is optimized to additionally minimize that probability. The details of OFM vary between different systems. Here developed OFM is tailored to describe the temperature fluctuations coupled with the electric current, so that the dynamical characteristic (temperature) of fluctuations satisfies the heat transfer equation.

The analysis below shows that hot spot instabilities evolve in a manner of phase transformations, either by nucleation or similar to spinodal decomposition affecting the entire area. The nucleation scenario of such instabilities in uniform systems was established earlier based on general phenomenological analysis.¹

One aspect of the hot spot phenomenon is that it is related to the underlying cylinder shaped filament regions of increased temperature and conductivity across the structure. The possibility of current filamentation in semiconductors has been long known; here we mention the seminal work in Refs. 14 and 15, and comprehensive modern analysis in Ref. 16 containing references to many other publications. A number of straightforward dynamical models are based on the coupled differential equations of heat transfer and electronic transport, the latter possessing certain features conducive of instabilities, such as, e. g. nonlinear electron transport related to electron system overheating, impact ionization or electroacoustic effects. While these models do not explicitly describe nonuniform systems, some of their results will be compared here to that of the present consideration in the limiting case of very weak disorder.

This paper is limited to a general theoretical analysis; possible applications of the coupled electron-heat transport will be presented in more appropriate journals. We refer to a recent monograph 17 for many practically important cases. The relevant observations are found with bipolar transistors¹⁷⁻²¹, other metal-insulator-semiconductor structures,²²⁻²⁷ nanoscale transistors,²⁸ graphene transistors,²⁹ and thin-film photovoltaics.^{30-32,35} In these applications, the phenomenon under consideration was labeled as thermal runaway, or hot spot, or (reversible) thermal breakdown. It can be detrimental to the corresponding device operations leading to their irreversible degradation in hot spots via local shunting, burning, or melting; hence, significance for device reliability.

The paper is organized as follows. Sec. II introduces the basic equations describing the coupled electron-heat transport in a non-uniform system. To better explain the essence of OFM and subsequent results, two toy models are considered in Sec. IV. Relation to the theory of heat explosions is discussed in Sec. V. Sec. VI, presents a modification of OFM describing saddle points through which the system evolves into thermally nonuniform state. The OFM functional is optimized in Sec. VII through direct variational procedure. The steady state rate of hot spot nucleation is estimated in Sec. VIII. Finally, Sec. IX presents general discussion and conclu-

sions.

II. COUPLED ELECTRON AND HEAT TRANSPORT IN A DISORDERED SYSTEM

The Joule power density is given by

$$P = P_0 \exp(-E/kT), \quad P_0 = \mathcal{E}^2 \sigma_0 \exp\left(-\frac{\bar{E}}{kT}\right). \quad (1)$$

Here $\mathcal{E} = V/h_0$ is the electric field strength where h_0 is the distance between the electrodes (see Fig. 1). σ_0 is the pre-exponential of conductivity,

$$\sigma = \sigma_0 \exp[-(\bar{E} + E)/kT]$$

with \bar{E} being the average activation energy, k is the Boltzmann's constant, and T is the local temperature. The random part of activation energy, E has zero average, $\langle E \rangle = 0$ and a finite dispersion $\langle E^2 \rangle = B$. It is characterized by the correlation function

$$\langle E(\mathbf{r}, z) E(\mathbf{r}', z') \rangle = Bv\delta(\mathbf{r} - \mathbf{r}')\delta(z - z'). \quad (2)$$

Here the radius vector \mathbf{r} lies in the film plane, z is the transversal (across the film) coordinate, $\delta(\mathbf{r})$ is the two-dimensional delta function implying zero correlation radius disorder. The minimum volume v is determined by the physical nature of fluctuations. For example, its characteristic linear scale $a_0 \sim v^{1/3}$ (likely in sub-micron range) can be given by the screening radius or the grain size, or other length, below which the system parameters do not vary significantly. v is introduced to give B the dimensionality of the square of energy and the meaning of the dispersion of random energies E .

Local elements of the system interact through heat transfer described by the standard equation

$$\chi \nabla^2 T + P(\mathbf{r}) = 0 \quad (3)$$

where χ is the thermal conductivity and the Laplacian ∇^2 is three dimensional, and χ is coordinate independent. The power generation density is a sum of average and random contributions,

$$P = \langle P \rangle + P^{(1)}, \quad \langle P \rangle \equiv P_0 \left\langle \exp\left(-\frac{E}{kT}\right) \right\rangle.$$

where

$$P^{(1)} = P_0 \exp\left(-\frac{E}{kT}\right) - \langle P \rangle. \quad (4)$$

Eq. (3) assumes the steady state heat transfer. The assumption of stationary states is common to all known cases of OFM. The problem under consideration, however, is different with respect to the notion of stationary fluctuations. Since the instability evolves in a fashion of phase transitions, the stationary solutions of Eq. (3) can

only describe saddle points in the parameter space. The temperature fluctuation δT becomes time dependent in the proximity of each of such point, described by

$$-C\delta T/\tau = \chi\nabla^2 T + P(\mathbf{r}) \quad (5)$$

in the relaxation time approximation, where C is the specific heat. The fluctuation decay will correspond to positive, while fluctuation growth (instability) to negative values of τ ; this criterion is used in Sec. VII below.

III. LINEAR APPROXIMATION: NO-BREAKDOWN REGIME

For completeness, consider briefly a trivial situation where the disorder B and temperature fluctuations δT are small enough to allow the linearization

$$P = P_0 \left[1 - \frac{E(\mathbf{r}, z)}{kT_0} + \frac{\bar{E}}{kT_0^2} \delta T(\mathbf{r}, z) \right], \quad z < h_0, \quad (6)$$

where T_0 is the average temperature. For simplicity, consider the probabilistic distribution of temperature fluctuations averaged over the film thickness,

$$\delta\tilde{T} = \frac{1}{h} \int_0^h \delta T(\mathbf{r}, z) dz. \quad (7)$$

that turns out to be almost identical to that of δT .

Substituting the linear approximation of Eq. (6) and performing averaging in Eq. (3) yields

$$\nabla_r^2 \delta\tilde{T} - \frac{1}{r_0^2} \delta\tilde{T} = u(\mathbf{r}). \quad (8)$$

Here ∇_r^2 is the two-dimensional Laplacian,

$$\frac{1}{r_0^2} \equiv \frac{P_0 \bar{E} h_0}{\chi k T_0^2 h}, \quad u(\mathbf{r}) \equiv \frac{P_0}{\chi k T_0 h} \int_0^{h_0} E(\mathbf{r}, z) dz. \quad (9)$$

The solution to Eq. (8) has the form

$$\delta\tilde{T}(\mathbf{r}) = (-1/4) \int d^2 r' u(\mathbf{r}') H_0^{(1)}(i|\mathbf{r} - \mathbf{r}'|/r_0) \quad (10)$$

where $H_0^{(1)}$ is the Hankel function.

The quantity in Eq. (10) represents a sum of large number of random contributions and, according to the central limit theorem, is a random quantity itself with the Gaussian probability distribution. Its dispersion $\langle (\delta\tilde{T})^2 \rangle$ is given by

$$\begin{aligned} & \frac{1}{16} \int_0^\infty d^2 r' d^2 r'' H_0^{(1)}\left(\frac{ir'}{r_0}\right) H_0^{(1)}\left(\frac{ir''}{r_0}\right) \langle u(\mathbf{r}') u(\mathbf{r}'') \rangle \\ &= \frac{\pi P_0 B v}{4\chi \bar{E} k h}. \end{aligned} \quad (11)$$

Here we have taken into account Eq. (2) and the value⁴⁷ of the integral $\int_0^\infty [H_0^{(1)}(x)]^2 x dx = 2$.

We conclude that the temperature fluctuations are characterized by the radii of r_0 and the Gaussian distribution,

$$\rho(\delta\tilde{T}) \propto \exp\left(-\frac{\delta\tilde{T}^2}{\delta T_0^2}\right) \quad \text{with} \quad \delta T_0^2 = \frac{\pi P_0 B v}{4\chi \bar{E} k h}. \quad (12)$$

A similar result can be obtained for the true (not z -averaged) temperature fluctuations δT . The only difference is that the Green function $-H_0^{(1)}(i|\mathbf{r} - \mathbf{r}'|/r_0)/4$ must be replaced by a rather cumbersome series (see e. g. Refs. 33, p. 144 and 34) including z -dependent trigonometry functions in combination with Bessel functions of r/r_0 . As a result, δT_0^2 remains the same parametrically with a numerical coefficient approximately equal to 0.7 instead of 1/4 in Eq.(12).

The important point is that the above linear approximation does not account for positive feedback of temperature fluctuations on transversal conduction and thus the disorder remains fixed and temperature independent. While this restriction eliminates the possibility of thermal breakdown (which is the main topic here), the results of this section can still be applicable to the case of very small currents and fluctuations used e. g. in thermography diagnostics.^{35,49}

IV. TOY MODELS

Because the regular OFM below is mathematically cumbersome, it is illustrated here with simplified (toy) models. One of them concentrates on the case when there is no positive feedback on conductivity by local heating. Another one deals with a homogeneous system and concentrates on the positive feedback.

A. Conductive filaments through an insulating film

Consider a two phase structure where transversal current flows through conductive filaments in an insulating host of thickness h_0 sandwiched between two equipotential electrodes. The structure is characterized by the average transversal conductivity $\bar{\sigma}$ due to filaments of average concentration \bar{n} per area. Local fluctuations δn in their concentration result in the corresponding conductivity fluctuations $\delta\sigma = \bar{\sigma}\delta n/n$. Since the filaments generate Joule heat, they create fluctuations δT in temperature; the tail of probabilistic distribution of δT is found below.

Consider a cylinder shaped region of radius a perpendicular to the electrodes where the characteristic fluctuation in filament concentration is δn . The Gaussian probability of such a fluctuation is estimated as

$$\exp\left[-\frac{(\delta n)^2 a^2}{\bar{n}}\right] = \exp\left[-\bar{n} a^2 \left(\frac{\delta\sigma}{\bar{\sigma}}\right)^2\right] \equiv \exp(-S) \quad (13)$$

S can be optimized with respect to a after $\delta\sigma$ is expressed via δT and a .

The heat flux through the cylinder base and side surfaces is estimated as $\chi[(\delta T/h_0)a^2 + (\delta T/a)h_0a]$ to within the accuracy of numerical multipliers of the order of unity in front of each of the terms. Equating it to the fluctuation of power $V^2a^2\delta\sigma/h_0$ inside the cylinder yields the temperature fluctuation

$$\delta T = \frac{V^2\delta\sigma}{\chi} \frac{a^2}{a^2 + h_0^2}. \quad (14)$$

Expressing $\delta\sigma$ from Eq. (14) and substituting it into Eq. (13) yields

$$S = \bar{n}a^2 \left(\frac{\delta T \chi}{V^2\bar{\sigma}} \right)^2 \left(1 + \frac{h_0^2}{a^2} \right)^2. \quad (15)$$

Following the OFM approach, we optimize the exponent S with respect to the fluctuation radius a , i. e. $dS/da = 0$, which gives $a = h_0$. Substituting $a = h_0$ back into Eq. (15) yields the optimum exponent of probability,

$$S_{opt} = \left(\frac{\delta T}{\delta T_0} \right)^2 \quad \text{where} \quad \delta T_0 \equiv \frac{V^2\bar{\sigma}}{\chi h_0 \sqrt{\bar{n}}} \quad (16)$$

again to the accuracy of numerical multipliers.

The preexponential is roughly estimated by dividing the entire area into elemental domains of area h_0^2 each and noticing that $\exp(-S_{opt})$ describes the probability of a desired fluctuation with temperature excess δT in a given domain. Therefore, the concentration of such fluctuations is estimated as $h_0^{-2} \exp(-S_{opt})$.

Two features should be noted. First, OFM concentrates on the exponent of probability, largely neglecting the pre-exponential factors (although they can be estimated as well). Secondly, it optimizes that exponent in order to find the most likely disorder configuration providing the desired fluctuation characteristic of interest. Its applicability is limited to the region of non-overlapping fluctuations.

A possible application of this toy model might be a system of multiple shunting metal chains formed in dielectric or solid electrolyte films considered for nonvolatile memory; see e.g. Refs. 48 and references therein.

B. Homogeneous films

Consider, in the linear approximation, a relatively small temperature fluctuation δT in a cylinder region of radius a and height h_0 , setting

$$\frac{1}{T} \approx \frac{1}{T_0} - \frac{\delta T}{T_0^2}. \quad (17)$$

Neglecting (for simplicity) heat transfer through the cylinder bases and using

$$\delta\sigma = \bar{\sigma} \exp\left(\frac{\delta T \bar{E}}{kT_0^2}\right),$$

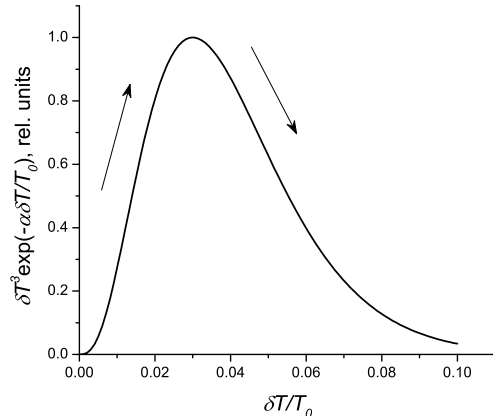


FIG. 2: Effective barrier for nucleation of hot spots corresponding to the numerical value $\alpha = \bar{E}kT_0 = 10$. Arrows show a pathway of hot spot nucleation.

Eq. (14) reduces to the form

$$\delta T = \frac{V^2\bar{\sigma}}{\chi} \frac{a^2}{h_0^2} \exp\left(\frac{\delta T \bar{E}}{kT_0^2}\right). \quad (18)$$

For a system in equilibrium, the probability of temperature fluctuation δT in volume $\delta V = \pi a^2 h_0$ is given by the expression³⁶

$$\exp[-C^{(v)}\delta V(\delta T)^2/kT^2]$$

where $C^{(v)}$ is the specific heat per volume. Expressing a^2 from Eq. (18) gives the *equilibrium distribution function* $\bar{f}(\delta T) \propto \exp[-S(\delta T)]$ with

$$S(\delta T) = -\frac{\pi C^{(v)} h_0^3 \chi}{2kT_0^2 V^2 \bar{\sigma}} \delta T^3 \exp\left(-\frac{\delta T \bar{E}}{kT_0^2}\right). \quad (19)$$

It follows from Eq. (19) that the equilibrium distribution is a minimum at $\delta T_c = kT^2/3\bar{E}$ where the product $\delta T^3 \exp(-\delta T \bar{E}/kT^2)$ is a maximum. On intuitive grounds, that minimum can be interpreted as the result of increase free energy at $\delta T = \delta T_c$: This is tantamount to a barrier in the system free energy at $\delta T = \delta T_c$: the probability of fluctuations first exponentially decreases as δT grows below δT_0 and then decreases when δT exceeds δT_c . Such a behavior is obviously similar to that known in nucleation phenomena^{36,44,45} (where the barrier is a function of the nuclear radius) and small polaron collapse⁴⁶ (where the barrier is a function of dilation). The instability point corresponds to a relatively very small temperature increase $\delta T_c = (kT_0/3\bar{E})T_0 \ll T_0$ in systems with high enough activation energies, say, $\delta T_c \lesssim 0.01T_0 \sim 3$ centigrade.

Based on that analogy, the exponent of probability of the thermal breakdown is given by $S(\delta T_c)$, that is, to the

accuracy of numerical multipliers,

$$S(\delta T_c) = \frac{k^2 T_0^3 C^{(v)} h_0^3 \chi}{\bar{E}^3 V^2 \bar{\sigma}}. \quad (20)$$

This approach will be made more consistent in Sec. VIII.

Note that the probability exponent optimization here results not in a minimum, but rather a maximum; it may turn into a saddle point in a parameter space of higher dimensionality as will be explicitly shown next. Another conclusion is that a positive feedback alone makes the instability possible regardless of the degree of disorder in the system.

V. DYNAMICAL MODELS AND HEAT EXPLOSIONS

In dynamical models^{15,16} the filament is described by the system of coupled differential equations for heat transfer and electronic transport. For the case under consideration and assuming uniform systems, they reduce to a single equation

$$-C\partial\delta T/\partial t = \chi\nabla^2 T + P_0 \exp(\gamma\delta T), \quad \gamma = \bar{E}/kT_0^2 \quad (21)$$

where t is time and we have used the linearization (17). While this equation has not been often considered with semiconductors, it has a long history describing thermal explosions in combustion. Comprehensive reviews of earlier work is given in Refs. 37,38; a short description included in a canonical text 39 (p. 199), and a review of modern applications⁴⁰ is available.

With combustion, the instability takes place when the rate of heat generation is faster than the rate of heat removal by the cooling system, thus leading to a continuous rise in the reactor temperature with a consequent acceleration of the reactions, leading eventually to explosion. A concept of hot spots as local regions quickly raised to high temperatures was developed⁴¹ (the production of such regions has been attributed to various causes) that has some similarity with the present work. These spots are characterized by the dimensionless local overheat

$$\Theta_0 = \frac{\delta T \bar{E}}{kT_0^2} \quad (22)$$

and the criticality parameter

$$\delta_c = \frac{h^2 P_0 \bar{E}}{\chi k T_0^2} \quad (23)$$

where h is the linear size of the spot. We note that the criticality parameter δ_c appears with all known treatments of thermal explosions.^{37,38,40}

For the case of hot spots, δ_c was derived as a function of Θ_0 , such that the hot spot with a given overheat Θ_0 will grow when δ_c exceeds the value of that function. The latter has different shapes^{41,42} for different geometries (slab, cylinder, sphere – not limited to the electric

connectivity condition specific to the current analysis). For example, the slab geometry is characterized by

$$\ln \Theta_0 = \frac{\delta_c}{4} + \frac{1}{2} \ln \frac{4\pi}{\delta_c}. \quad (24)$$

It was found that the hot spot instability occurs starting from large enough $\Theta_0 \approx 4 - 5$; this translates into corresponding inequality on δ_c . We will see that our results below (see Sec. VII C) are consistent with these findings of the heat explosion theory.

VI. OPTIMUM FLUCTUATION METHOD

The subtlety of the optimum fluctuation method is in how it treats the disorder induced distribution of temperature $T(\mathbf{r})$ (or wave function for the standard case of energy spectra in systems with random potential energy). Namely, $T(\mathbf{r})$ is considered a smooth 'optimum' function approximating the temperature distribution for the most likely disorder configuration responsible for any desired temperature fluctuation. It remains arbitrary (yet fixed) in the course of the analysis and is determined later by the condition of the maximum of the probability. Such optimization benefits from the known property of variational techniques that any inaccuracy in the trial function translates into a higher order inaccuracy in the corresponding functional.

In what follows we take into account only exponentially strong activation factor ignoring all possible pre-exponentials found with temperature dependent conductivity in semiconductors. This simplification simultaneously determines the accuracy of our analysis where all the pre-exponential factors are replaced with their averages. In particular, this analysis is limited to the case of strong enough fluctuations beyond the linear approximation for $P[\delta T(\mathbf{r})]$.

A. OFM equations

The heat transport equation (3) can be treated as an extremum of the functional

$$F = \int d^3 r \left[\frac{\xi}{2} (\nabla T)^2 - P(\mathbf{r}) \right] \quad (25)$$

where the pre-exponential factor $(E + \bar{E})/T^2$ [generated by variation of P in Eq. (1)] is approximated by its average,

$$\xi \equiv \chi \langle (\bar{E} + E)/kT^2 \rangle. \quad (26)$$

The latter functional can be presented as

$$F = \int d^3 r \left[\frac{\xi}{2} (\nabla T)^2 - \langle P \rangle \right] - Z \quad (27)$$

where T depends on coordinates and random variable Z is defined by

$$Z = \int d^3r P^{(1)}(\mathbf{r}) \quad (28)$$

We note that the approximation of averaged preexponential in Eq. (25) is justified when the exponent in $P \propto \exp[(E + \bar{E})/kT]$ is large enough, $(E + \bar{E})/kT \gg 1$. This takes place indeed for large activation energies assumed here. In addition, we will see that $E/kT \sim S \gg 1$ in significant range where S is the exponent of probability of filamentation $\exp(-S)$ [see the remark after Eq. (60)].

OFM suggests that the dispersion of random variable Z can be found as

$$D = \langle Z^2 \rangle = \int \int d^3r d^3r' \langle P^{(1)}(\mathbf{r}) P^{(1)}(\mathbf{r}') \rangle \quad (29)$$

where the average in the integrand is evaluated under the condition of a fixed (yet arbitrary) function $T(\mathbf{r})$. The integral in Eq. (28) contains a large number of random contributions. Therefore, according to the central limit theorem, Z is described by Gaussian statistics, i. e. its probabilistic distribution

$$g(Z) \propto \exp[-S(Z)], \quad S = \frac{Z^2}{2D}. \quad (30)$$

A comment is in order regarding the latter statement of Gaussian statistics for random quantity Z . According to the definition in Eq. (28), the kernel of Z is exponential in Gaussian random variable E . That exponent $\exp[-E(\mathbf{r})/kT]$ is by no means a Gaussian variable. Yet, the values of that variable at different points \mathbf{r} are statistically independent due to the property in Eq. (2). Also, it has a finite average,³⁶

$$\langle \exp(E/kT) \rangle = \exp[\langle (E/kT)^2 \rangle / 2] \quad (31)$$

and a finite dispersion $\exp[2\langle (E/kT)^2 \rangle] - \exp[\langle (E/kT)^2 \rangle]$. These properties are sufficient to state that a sum of large number of such *non Gaussian* random terms $\exp(E/kT)$ representing the functional Z will obey Gaussian statistics.⁴³

The maximum probability fluctuation corresponds a stationary point of $S(Z)$ under the additional condition of Eq. (27). Finding such a conditional extremum is tantamount to finding an unconditional extremum of a functional

$$\Phi = \frac{Z^2}{2D} - \lambda F \quad (32)$$

where λ is the undetermined Lagrange multiplier. λ is then found from the additional condition of a certain predetermined maximum temperature in the the optimum fluctuation region.

The functional Φ must be optimized with respect to the disorder configuration $E(\mathbf{r})$ and the field $T(\mathbf{r})$. Because the former appears only with the integral Z , the

optimization can be more conveniently conducted with respect to Z and $T(\mathbf{r})$. The corresponding equations are

$$\frac{Z}{D} + \lambda = 0 \quad (33)$$

and

$$-\frac{Z^2}{2D^2} \frac{\delta D}{\delta T} + \lambda \xi \nabla^2 T + \lambda P_0 \left(\frac{\bar{E}}{kT^2} - \frac{\langle E^2 \rangle}{k^2 T^3} \right) \exp \left(\frac{\langle E^2 \rangle}{2k^2 T^2} \right) = 0. \quad (34)$$

Here we have again taken into account the property in Eq. (31) for a Gaussian random variable E/kT . Using Gaussian statistics in combination with the concept of thermally activated current assumes the inequality

$$\frac{\bar{E}}{kT} \gg \frac{\langle E^2 \rangle}{k^2 T^2}. \quad (35)$$

Allowing the opposite inequality would lead to the physically unacceptable feature that the typical fluctuation current exponentially decreases with temperature.

Substituting Eq. (33) into Eqs. (30) and (34) yields the equations determining the optimum fluctuation temperature field $T(\mathbf{r})$ and its corresponding probability exponent,

$$-\frac{\lambda D}{2} \frac{\delta D}{\delta T} + \xi \nabla^2 T + P_0 \left(\frac{\bar{E}}{kT^2} - \frac{\langle E^2 \rangle}{k^2 T^3} \right) \exp \left(\frac{\langle E^2 \rangle}{2k^2 T^2} \right) = 0, \quad (36)$$

$$S = \frac{D\lambda^2}{2}. \quad (37)$$

To evaluate $\delta D/\delta T$ that is the variational derivative of the integrand in Eq. (29) we use again the property of averaging of a Gaussian random variable $E(\mathbf{r})$. The integrand in Eq. (29) becomes

$$P_0^2 \exp \left[\frac{\langle E^2 \rangle}{(kT)^2} \right] \int d^3r' \left\{ \exp \left[\frac{\langle E(\mathbf{r})E(\mathbf{r}') \rangle}{k^2 T(\mathbf{r})T(\mathbf{r}')} \right] - 1 \right\}.$$

For the case of delta correlated disorder in Eq. (2), the latter expression can be approximated as

$$P_0^2 s h_0 \exp \left[\frac{2B}{(kT)^2} \right]. \quad (38)$$

Substituting the result of differentiation [together with Eq. (33)] into Eq. (34) leads to a closed form single equation for the optimum fluctuation $T(\mathbf{r})$. That equation is not very useful practically because of its rather complex form. The problem becomes easier when presented in the form of functional subject to direct optimization with respect to $T(\mathbf{r})$. That functional is given by

$$J = \int d^3r F[T(\mathbf{r})] \quad (39)$$

where

$$F = \frac{\xi}{2}(\nabla T)^2 - P_0 \exp\left[\frac{B}{2(kT)^2}\right] - \lambda P_0^2 v \exp\left[\frac{2B}{(kT)^2}\right] \quad (40)$$

Note that, to the accuracy of the factor of $-\lambda$, the third term in the functional J [corresponding to the third term in Eq. (40)] is twice the probability exponent S .

B. OFM saddle points

While optimization of functional J remains to be implemented, the nature of its stationary points can be determined already here. Assuming a trial function $T = T(r/a)$ and changing variable $r \rightarrow r/a$, J can be presented in the form

$$J = J_1 + a^2 J_2$$

where J_1 and J_2 do not depend on a . Treating a^2 as a variational parameter, leads to the conclusion that $d^2 J/d(a^2)^2 = 0$ at the stationary points where $J_2 = 0$. Hence, they represent inflection points rather than minima. In a higher dimension parameter space including the temperature fluctuation amplitude, these points can only be saddles.

The saddle point solutions require a different interpretation of OFM results. From the physical standpoint, some (but not all) of their related configurations should appear with certainty, i. e. with $S = 0$, since they are not steady state, and thus are to be passed inevitably sooner or later. From that perspective, they are similar to the barriers of classical nucleation theory^{36,44,45} or small radius acoustic polaron formation.⁴⁶ For example, the OFM saddle points in the surface $J(a, T)$ can physically describe critical radii $a(T)$ separating the regions of spontaneous decay from that of spontaneous growth of fluctuations. This similarity to the nucleation theory will be made explicit in Sec. VII.

Note that the fact of probability exponent S vanishing at the OFM saddle points, does not compromise OFM as long as the corresponding fluctuations remain strongly localized and do not overlap. The latter conditions do not necessarily invoke $S \gg 1$ (unlike the conclusion of Sec. IV where all the fluctuations simultaneously coexist), since the saddle point events are not steady state taking place at different time instances.

Consider the configurational probability exponent S in a certain proximity of a saddle point $S = 0$. We denote $\delta T_0(\mathbf{r})$ the temperature distribution in the optimum fluctuation corresponding to $S = 0$. If the optimum fluctuation $\delta T(\mathbf{r})$ is different from $\delta T_0(\mathbf{r})$, one can extend

$$S = \int d^3 r \left(\frac{\delta^2 S}{2\delta T^2} \right)_0 [\delta T(\mathbf{r}) - \delta T_0(\mathbf{r})]^2, \quad (41)$$

where the integrand is positive. The equilibrium distribution function of such fluctuations is given by

$$\bar{f}(\delta T) = \bar{f}_0 \exp \left\{ -\frac{C^{(v)}}{2kT_0^2} \int d^3 r [\delta T(\mathbf{r})]^2 - S \right\} \quad (42)$$

Here \bar{f}_0 is the preexponential factor and we have taken into account the expression for the probability of equilibrium temperature fluctuation δT in volume δV mentioned in Sec. IV B.

It is seen from Eq. (42) that \bar{f} is a minimum at some δT different from δT_0 . Following the Fokker-Planck approach to nucleation (Zeldovich' theory; see e. g. Chapter XII in Ref. 44) and in agreement with the qualitative analysis in Sec. IV B, that minimum determines the nucleation barrier and rate. This approach will be implemented in Sec. VIII below upon determining the parameters of OFM solutions $\delta T(\mathbf{r})$.

VII. DIRECT VARIATIONAL PROCEDURE

A. Trial function and functional

Here we implement a direct variational procedure of optimization of the functional J using the simplest trial function

$$\frac{\delta T}{T_0} = \theta \left(1 - \frac{r}{\tilde{a}h}\right) \left(1 - \frac{z}{h}\right) \quad \text{when } \delta T > 0 \quad (43)$$

that is zero outside of the domain $r < \tilde{a}h$, $z < h$. Here r and z are the radial and transversal (across the film) coordinates. θ and \tilde{a} are the two variational parameters, defined as being dimensionless to make the resulting equations more compact. In particular, θ is the amplitude excess temperature in fluctuation measured in the units of the average temperature T_0 , and \tilde{a} has the meaning of the fluctuation radius measured in the units of structure thickness h .

Note that integration over the transversal (z) coordinate extends over the entire structure thickness ($2h$) for the first term in Eq. (40), while the second and third terms must be integrated only over the active layer thickness ($2h_0 \ll h$) where the power is generated. The constraint $t = 0$ at $z = h$ correctly reflects the boundary condition of a constant temperature at the interface (see Fig. 1). Furthermore, we assume fluctuation to be relatively small, allowing the linearization in Eq. (17). Also, we note that it would be more natural to use a trial function quadratic in z , so $d\delta T/dz = 0$ at $z = 0$ reflecting the system symmetry. We have checked however that such a modification does not have any significant effect on the functional and final results; for example, $(\tilde{a}^2 + 2)$ in Eq. (44) changes to $[(2/3)\tilde{a}^2 + 1.6]$. Such insensitivity is well known in variational problems, leading e.g. to only $\sim 10\%$ error in the energy of harmonic oscillator evaluated with the trial wave function linear in coordinate (see e.g. Ref. 50, p.95).

Substituting Eq. (43) and carrying out the integration reduces J to the form

$$\frac{12\alpha^2 J}{\xi T_0^2 \pi h} = (\tilde{a}^2 + 2) x^2 - \beta \tilde{a}^2 \Phi(x) - \lambda \beta' \beta \tilde{a}^2 \Phi \left(x \frac{\alpha'}{\alpha} \right) \quad (44)$$

where

$$x = \alpha\theta \quad \text{and} \quad \Phi(x) = \frac{\exp(x) - x - 1}{x^2}. \quad (45)$$

Here we have introduced the parameters defined as

$$\alpha = \frac{\bar{E}}{kT_0} - \frac{B}{(kT_0)^2}, \quad \alpha' = 2 \left[\alpha - \frac{B}{(kT_0)^2} \right] \approx 2\alpha,$$

$$\beta = \frac{24hh_0P_0\alpha^2}{\xi T_0^2} \exp \left[\frac{B}{2(kT_0)^2} \right], \quad \beta' = P_0v \exp \left[\frac{3B}{2(kT_0)^2} \right].$$

The inequality in Eq. (35) limits them to $\alpha \gg 1$. In integrating over z in Eq. (44), we have assumed a practically important case when the semiconductor layer is very thin, $\alpha\theta h_0/h \ll 1$, and calculations are simpler.

Because eventually we consider $\theta = x/\alpha$ an independent *given* variable, the optimization conditions $\partial J/\partial \tilde{a}^2 = 0$ and $\partial J/\partial x = 0$ must be used to solve for \tilde{a}^2 and λ . In agreement with the conclusion of Sec. VI, the stationary points found from the optimization are saddle points. This is seen from the sign of the determinant

$$\frac{\partial^2 J}{(\partial \tilde{a}^2)^2} \frac{\partial^2 J}{(\partial \theta)^2} - \left[\frac{\partial^2 J}{(\partial \tilde{a}^2) \partial \theta} \right]^2 < 0$$

identifying the stationary points as saddles.⁵¹

B. Regional approximations

Consider the results of optimization of the functional J for three complimentary regions.

1. Weak fluctuations, $x \ll 1$

Assuming $x \ll 1$ reduces $\Phi(x)$ in Eq. (44) to $\Phi(x) \approx 1/2 + x/6 + x^2/24$, which significantly simplifies the optimization. This leads to the physically unacceptable solution with $\tilde{a}^2 = -32/(8 + \beta) < 0$.

2. Moderate fluctuations, $x \sim 1$

It is straightforward to verify that the interpolation $\Phi(x) = 1/2 + x^2/6$ holds to the accuracy of several percent for intermediate $x \leq 4$. Using that interpolation, the optimization of J results in the physically inconsistent solution as well, $\tilde{a}^2 = -[12 + 16(\alpha\theta)^2]/(6 + 3\beta)$.

3. Strong fluctuations, $x \gg 1$

Acceptable solutions with $\tilde{a}^2 > 0$ exist in the case of $\alpha\theta \gg 1$ (and yet $\alpha\theta h_0/h \ll 1$) where one can approxi-

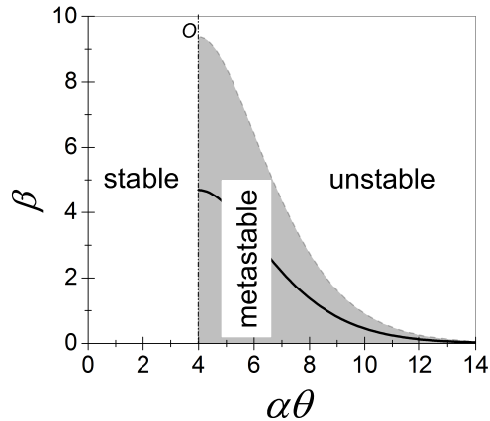


FIG. 3: Phase diagram for a thin film structure with transversal current vs. power density (parameter β) and local temperature increase (parameter $\alpha\theta$). Region to the left of the line $\alpha\theta = 4$ represents the stable phase where local temperature fluctuations decay making thermal breakdown impossible. The gray colored region below the line of solution of Eq. (50), represents metastable state corresponding to the saddle points, through which thermal breakdown nucleates locally. The solid curve in that region is a solution of Eq. (51); it corresponds to the most likely nucleation events, for which $S = 0$ in Eq. (46). The region above the line of solution of Eq. (50) represents the globally unstable state of the system.

mate $\Phi(x) = \exp(x^2)/x^2$. This yields

$$\begin{aligned} \lambda &= \frac{(\alpha\theta)^4 - \beta \exp(\alpha\theta)}{\beta\beta' \exp(2\alpha\theta)}, \\ \tilde{a}^2 &= \frac{4(\alpha\theta)^3}{2(\alpha\theta)^4 - \beta \exp(\alpha\theta)}, \\ S &= S_0 \frac{\theta[(\alpha\theta)^4 - \beta \exp(\alpha\theta)]^2 \exp(-2\alpha\theta)}{2(\alpha\theta)^4 - \beta \exp(\alpha\theta)} \end{aligned} \quad (46)$$

where

$$S_0 \equiv \frac{\pi(\xi T_0^2)^2 \exp[-2B/(kT_0)^2]}{288P_0^2vh_0} \quad (48)$$

and

$$\theta_{c1} < \theta < \theta_{c2}, \quad (49)$$

with θ_{c1} and θ_{c2} being the two solutions of the transcendental equation

$$2(\alpha\theta)^4 - \beta \exp(\alpha\theta) = 0. \quad (50)$$

The condition

$$(\alpha\theta)^4 - \beta \exp(\alpha\theta) = 0 \quad (51)$$

describes the points where $S = 0$ and thus nucleation of hot spots takes place, according to the discussion in

Sec. VI B. These points all fall within the domain of physically acceptable solutions in Eq. (49). Also, it follows from comparison of Eqs. (50) and (51) that the radii of the corresponding stationary fluctuation states remain finite as required by OFM.

Because $(\alpha\theta)^4 \exp(-\alpha\theta)$ is a maximum at $\alpha\theta = 4$, Eq. (51) has solutions when

$$\beta \leq \beta_c = \left(\frac{4}{[e]}\right)^4 \approx 4.7 \quad (52)$$

where $[e]$ stands for the base of natural logarithms. Close to that threshold value, the dependence $t(\beta)$ takes the form

$$\alpha\theta \approx \alpha\theta_0 = 4 + \sqrt{\beta_c - \beta} \quad \text{when} \quad \beta_c - \beta \ll 1. \quad (53)$$

Another branch of $\alpha\theta$ with the minus sign before the square root is ignored as belonging to the moderate fluctuation regime.

Alternatively, one gets from Eq. (51),

$$\alpha\theta \approx \alpha\theta_0 = \ln(1/\beta) \gg 1 \quad \text{when} \quad \beta \ll \beta_c. \quad (54)$$

This behavior corresponding to the far right part of the solid curve in Fig. 3 describes the low power regime.

C. Phase diagram

The complementary region to the left of the line $\alpha\theta = 4$ in Fig. 3 was characterized by the physically unacceptable solutions with $\tilde{a}^2 < 0$ (see Sec. VII B 1 and VII B 2). Here, we argue that that region represents the state where the system remains stable with respect to thermal fluctuations. A proof is achieved by including in the above analysis the term $-C\delta T/\tau$ from Eq. (5) describing the temporal behavior of fluctuation. It is straightforward to see that the unacceptable negative \tilde{a}^2 turn positive when $\tau > 0$, i. e. the corresponding fluctuations decay.

Alternatively, for the region above the curve $\beta = 2(\alpha\theta)^4 \exp(-x)$, adding the term with negative relaxation time $\tau < 0$ allows for positive \tilde{a}^2 . Therefore, the states in that region are globally unstable, i. e. they evolve into highly conductive high temperature states without any barrier. This is qualitatively similar to the phase transition scenario of spinodal decomposition,⁵² which is not described in the OFM framework.

Note the triple point O at $(\beta = 2\beta_c, \alpha\theta = 4)$ in Fig. 3 where all three phases coexist. It is straightforward to show that fluctuations $\delta\theta$ become increasingly strong in its proximity where

$$S = -\frac{S_0\beta^2\alpha}{(\alpha\theta_0)^5}(\alpha\theta_0 - 4)^2(\delta\theta)^2 \quad (55)$$

and $|\delta\theta| = |\theta - \theta_0| \ll \theta_0$. That property is similar as well to that of the standard phase transition phase equilibria.³⁶

We are now in a position to compare some of our results with the findings of heat explosion theory (Sec. V) based on the dynamical equation approach. The comparison is obviously limited to the assumption of uniform systems ($B = 0$ in all the above equations) underlying the heat explosion theory. Also, we should take into account the above used technical approximation $h_0 \ll h$ not immediately consistent with a single scale theory of heat explosion. In order to make the comparison possible we shall set in the above equations $h_0 = h$ hoping that they remain valid in the order of magnitude.

With the above in mind, we find the following correspondences. Our parameter β becomes, to the accuracy of numerical multipliers equal the criticality parameter in Eq. (23),

$$\beta = \frac{h^2 P_0 \alpha^2}{\xi T_0^2} = \delta_c,$$

where we have taken into account the definition of xi in Eq. (26). Our prediction that β needs to be higher than certain value in order to create instability is then consistent with that of thermal explosion theory.

Next, the product $\alpha\theta$ shown in Fig. 3 is related to the parameter Θ_0 in Eq. 22,

$$\alpha\theta = \Theta_0;$$

hence, our condition $\alpha\theta > 4$ becomes similar to the inequality on Θ_0 mentioned in Sec. V.

The latter relations make the coordinates $(\alpha\theta, \beta)$ in Fig. 3 identical to (Θ_0, δ_c) of the hot spot description⁴¹ in thermal explosion theory, although the shapes of the corresponding phase diagrams do not coincide. Note in this connection that the thermal explosion theory is not concerned at all with filament-like instabilities (since the requirement of electric current flow is of no significance there), and that the shape of diagram in Fig. 3 is strongly determined by its underlying limitations, such as e.g. $h_0 \ll h$.

D. Approximation of classical nucleation theory

The approximation of classical nucleation theory implies a narrow boundary region between the two phases and its related concept of surface energy. It can be attempted in the current framework by choosing a trial function

$$\frac{\delta T}{T_0} = \theta \begin{cases} 1 & \text{when } r < a, \\ (a+d-r)/d & \text{when } a < r < a+d, \\ 0 & \text{when } r > a+d \end{cases} \quad (56)$$

with $d \ll a$. As a result, the gradient term in Eq. (40) is determined by the contribution from a narrow layer of width d analogous to nucleus interfacial energy in functional J of Eq. (39). The procedure of optimization

becomes even simpler than that based on the trial function of Eq. (43). Omitting the details, the result is that the functional J has no stationary points when $d \ll a$. Hence, the approximation of interfacial energy does not apply to the case under consideration; the function in Eq. (43) remains more adequate.

VIII. STEADY STATE TRANSITION RATE

Consider the probability of thermal breakdown at a given power density P_0 described in terms of the parameter $\beta < \beta_c$. Using $\delta T(r, z)$ from Eq. (43) and expressions for \tilde{a} and S from Eq. (46), the equilibrium distribution function becomes

$$\bar{f}(\theta) = f_0 \exp \left[-\frac{\pi C^{(v)} h^2 h_0 \theta^2 \tilde{a}^2(\alpha\theta)}{3k} - S(\alpha\theta) \right]. \quad (57)$$

$S(\alpha\theta)$ is a maximum, $S = 0$, at the line shown in Fig. 3 and increases towards the boundary $\alpha\theta = 4$. However, given realistic parameters (see Sec. IX) that increase is not nearly as significant as the increase of the first term in the exponent in Eq. (57). As a result, $\bar{f}(\theta)$ has a sharp minimum at $\alpha\theta \approx 4$.

Following the known approach of nucleation theory⁴⁴ (mentioned in Sec. VIB above) consider a stationary Fokker-Planck equation

$$j = -B \frac{\partial f}{\partial \theta} + Af = \text{const} \quad (58)$$

for the 'kinetic' temperature distribution function $f(\theta)$. Here j is the flux in the temperature fluctuation (θ) space, D is the diffusion coefficient in that space; A is connected with D by a relationship which follows from the fact that $j = 0$ for the equilibrium distribution $f = \bar{f}$. Using the latter enables one to present the flux as $j = -B \bar{f}(\partial/\partial\theta)(f/\bar{f})$, and, hence, $f/\bar{f} = -s \int d\theta/B\bar{f} + \text{const}$. Finally, applying the boundary conditions $f \rightarrow 0$ when $t \rightarrow \infty$ and $f = \bar{f}$ when $\theta = 0$, yields

$$\frac{1}{j} = \int_0^\infty \frac{d\theta}{B\bar{f}}. \quad (59)$$

The integral is determined by a narrow proximity of the minimum of \bar{f} that gives the exponent of the transition rate.

To roughly evaluate the preexponential factor (without any knowledge of D) one can divide the entire area into a set of cells of characteristic linear size of the optimum fluctuation $\tilde{a}h$. Then the preexponential must be of the order of the rate of temperature variations $\kappa/(\tilde{a}h)^2$ in a cell where κ is the thermal diffusivity. This yields the steady state nucleation rate ($\text{cm}^{-2}\text{s}^{-1}$),

$$j \sim \frac{16\kappa}{h^4} \exp \left[-\frac{\pi C^{(v)} h^2 h_0 \theta^2 \tilde{a}^2(4)}{3k} - S(4) \right] \quad (60)$$

where $\tilde{a}^2(4) \equiv \tilde{a}^2(\alpha\theta = 4)$ and $S(4) \equiv S(\alpha\theta = 4)$ are given in Eq. (46). The power density enters this result through the parameter β in Eq. (48). Note that $S(4) \gg 1$, which inequality is consistent with the approximation of averaged preexponential in Eq. (25).

This result becomes more explicit for the case of low enough power when $\beta \exp(4) \ll 4$ in Eq. (46) and the absolute value of the exponent in Eq. (60) is estimated as

$$S \approx 8 \frac{C^{(v)} h^2 h_0}{\alpha^2 k} + 7 \cdot 10^{-6} \frac{(\xi T_0^2)^2 \exp[-2B/(kT_0)^2]}{\alpha h_0^2 s P_0^2}. \quad (61)$$

This is similar to the exponent in Eq. (20) emphasizing the important role of specific heat and rapidly decreasing with the power density. However it has a distinct feature of a lower boundary beyond which it cannot be further reduced even for very high power densities. It should be remembered however that high enough power densities are conducive to a different type of instability similar to the spinodal decomposition transformations as reflected in Fig. 3.

IX. DISCUSSION AND CONCLUSIONS

A. Numerical estimates

Assuming the typical semiconductor values,⁵³ one gets $\chi \sim 1 \text{ W/cm-grad}$ and $\bar{E}/T \sim 10 - 100$ for activation energies $\bar{E} \sim 1 \text{ eV}$ and $T \sim 100 - 500 \text{ }^\circ\text{K}$. This yields $\xi \sim 1 - 100 \text{ W/cm-grad}^2$, $\alpha \sim 10 - 100$.

For geometrical parameters, it is natural to assume $h_0 \sim 1 \mu\text{m}$, $s \sim 1 \mu\text{m}^2$, and $h \sim 10^{-4} - 10^{-1} \text{ cm}$. The current density in the range from $1 \mu\text{A/cm}^2$ to 1 A/cm^2 and electric fields $\mathcal{E} \sim 10^3 - 10^5 \text{ V/cm}$ are used in many device operations. The corresponding power densities are in the range from 1 mW/cm^3 to 10^5 W/cm^3 . The fluctuation strengths exponent $\exp[-2B/(kT_0)^2]$ can be evaluated as $\sim 0.001 - 1$ based on the observations of transversal currents through nonuniform Schottky barriers and thin film photovoltaics.⁵⁴ Finally, we use the thermodynamic parameters $C \sim 0.1 - 1 \text{ J/sm}^3\text{-}^\circ\text{C}$ and $\kappa \sim 0.1 - 1 \text{ cm}^2/\text{s}$. With the above parameters, the preexponential factor in Eq. (60) is estimated as $\sim 10^5 - 10^{13} \text{ cm}^{-2}\text{s}^{-1}$. Given that preexponential, the exponent in Eqs. (60) and (61) can be then within the range of experimentally important nucleation rates only for micron or sub-micron thin devices. Assuming greater thickness, say, $h \gtrsim 1 \text{ mm}$ makes the thermodynamic term proportional to C large enough to practically rule out the possibility of thermal breakdown mechanism under consideration.

However, semiconductor devices of modern electronics are often 10-100 nm thick (unless intended thermal sinks are used), and for them the thermodynamic fluctuation term in the exponent is not too large. For such structures, the second term in the nucleation rate exponents can be not terminally large for powers in the range $P_0 \gtrsim$

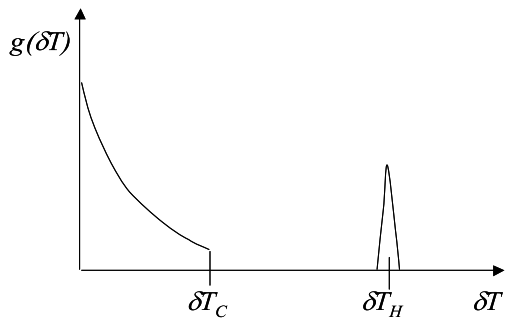


FIG. 4: Probability $g(\delta T)$ of hot spots vs. their excess temperature δT . The Gaussian tail at low δT is described in Sec. IV B. The critical overhear δT_c corresponds to the condition $\alpha\Theta = 4$ illustrated in Fig. 3. The high temperature peak at δT_H is determined by the processes of saturation of activated conduction and inter-spot interactions as explained in Sec. IX B; its width is due to disorder effects.

100 W/cm³. Overall, this makes the above considered mechanism realistic for structures in submicron region.

Finally, the minimum power density corresponding to the critical value of β in Eq. (52), above which the nucleation mechanism turns into that of global instability, can be estimated as $P_0 \gtrsim 10^{11}$ W/cm³. This range of power density is above practically all types of modern semiconductor devices, except maybe some cases of power electronics.

B. Discussion

The above consideration is limited to a basic instability triggered by Joule heat in combination with activated conduction. The instability is predicted to start under insignificant local overheats of several degrees. However, this analysis does not address the final parameters to which the instability can grow.

The 'stabilized' temperature excess δT_H in the developed filament (beyond the present theory framework) can be rather substantial. As pointed in Ref. 1, it can belong in the temperature range where the activated conduction saturates. That high temperature limit should not be mixed with the above predicted transition temperature excess, $\delta T_c \approx 4kT^2/\bar{E} \ll \delta T_H$ (corresponding to $\alpha\Theta \approx 4$), starting from which the instability evolves. This is illustrated in Fig. 4.

Furthermore, it is conceivable that the steady state high temperature local overhear δT_H cannot be determined by any extension of the present theory limited to noninteracting hot spots, even if activated conduction is allowed to saturate. The concentration of steady state hot spots at δT_H can significantly depend on their interaction. Indeed, the present theory predicts (Sec. VIII) that even at arbitrarily however low rates, the above de-

scribed instabilities will keep developing (maybe beyond the practically significant time intervals) to take over the entire structure area. This contradictory prediction is not unique of the system under consideration. It is known in the theory of phase transition where the nucleation stage is limited by various inter-nucleus interactions, such as competition for material, elastic stresses, etc. Similarly limiting interactions here will include competition of hot spots for the electric current, thermal fields by other filaments, etc. This analogy leads to the prediction of the growth and ripening stages of thermal breakdown kinetics, similar to that of the standard phase transitions;⁴⁴ a theory of such later stages of hot spot transformation remains to be developed.

While not related to structural transformations, the predicted local temperature increase can accelerate such transformations leading to permanent failures in the form of conducting pathways. Therefore, this mechanism can serve as a precursor to permanent structural failures. From that point of view, the above results on low temperature thermal breakdowns $\delta T_c \ll T$ point at high sensitivity of the fatal failure probability to the activation energy of conductivity and thermodynamic variables, particularly, specific heat, thickness, and thermal insulation.

The role of inactive (thermally insulating) layers exponentially reducing the thermal breakdown rates is due to the filament diameter increase with its length. As a result the thermal gradient in radial direction decreases suppressing the instability rate. This is consistent with the known practical solutions using substantial heat sinks attached to with submicron electronic devices in order to minimize their failure rates.

A more theoretical comment is in order regarding the relevance of the above OFM modification aimed at 'non-traditional' saddle type of stationary points. The underlying motivation was to relate localized temperature fluctuations with other known localized states in disordered systems. However the same basic equations as derived in Sec. VI could be obtained in the framework of instanton approach suitable for theoretical description of nucleation.⁵⁵⁻⁵⁷ That approach would start with the time dependent heat transfer equation leading to the variational problem for the exponent of probability $\exp[-R(T, t)]$ where t is time and R is related to the functional in Eq. (25), $R \propto \int^t F[T(t)]dt$. F remains a random functional to be additionally optimized to maximize the probability. That reduces the conditional variational problem for R to that of unconditional extremum in Eq. (32) yielding final expressions of OFM in Eq. (36).

The above theory has the following limitations. (1) The assumption of fixed voltage V across the film implying that the current I through the filament must be small enough, $IR_{sh} \ll V$ where R_{sh} is the sheet resistance of the conductive electrodes. (2) Simplification of uniform thermal conductivity may have noticeable quantitative ramifications, yet can hardly change the qualitative predictions. (3) The approximation of δ -correlated disorder, according to which the transversal conductiv-

ity must fluctuate across the distances smaller than the filament radius. The opposite regime of strongly correlated disorder can be readily described by the above results reduced to the case of homogeneous structures, in which then consider P_0 or $\bar{\sigma}$ as a random quantity varying over distances greater than the filament radius. (4) The optimum fluctuation method per se with accuracy limited to the probability exponent. (5) Inaccuracy of the direct variational procedure with a simplistic trial function remains unknown. Based on many similar examples, one can expect the results to be semi-quantitatively correct. (6) Limitation of small temperature fluctuations $\alpha\theta h_0/h \ll 1$, remains self-consistent as long as it is consistent with the final results for θ as it takes place in the above.

C. Conclusions

The following was shown.

- (i) Thin film semiconductor structures with activated transversal conduction are unstable with respect to reversible thermal breakdowns in the form of hot spots and their related current filaments.
- (ii) The instabilities evolve in a manner of phase transitions by either nucleation (at not too high power densities) or absolute instability similar to spinodal decomposition (above certain critical power density).
- (iii) The optimum fluctuation method can be modified to describe the saddle points, through which such transitions occur.
- (iv) The instabilities start with finite local temperature fluctuations that are smaller than the average temperature T_0 by the factor of kT_0/\bar{E} with \bar{E} being the average activation energy of electric conduction. The initial fluctuation radii are by the same factor smaller than the structure thickness.
- (v) The stable, metastable, and unstable phases of a thermally uniform system form a diagram (in variables power density – temperature) similar to the standard phase diagrams of phase equilibria, in particular, with fluctuations diverging towards the triple point.
- (vi) The steady state nucleation rate of hot spots exponentially depends on the material parameters, system geometry, and disorder strength.

The author hopes that this consideration can form a theoretical basis to analyze system failures in various structures of modern thin film devices; specific examples will be presented elsewhere.

Acknowledgments

This work was performed under the auspice of the NSF award No. 1066749. Discussions with I. V. Karpov, A. V. Subashiev, A. Vasko, and K. Wieland are greatly appreciated.

- ¹ A. V. Subashiev and I. M. Fishman, Sov. Phys. JETP **66**, 1293 (1987) [Zh. Eksp. Teor. Fiz., **93**, 2264 (1987)]
- ² I. M. Lifshitz, Adv. Phys. **13**, 483 (1964)
- ³ B. I. Halperin and M. Lax, Phys. Rev. **148**, 722 (1966); **153**, 802 (1967)
- ⁴ J. Zittarz and J. C. Langer, Phys. Rev. **148**, 741 (1966)
- ⁵ I. M. Lifshitz, S. A. Gredskul, and L. A. Pastur, *Introduction to the Theory of Disordered Systems* (Wiley, New York, 1987)
- ⁶ P. V. Meighem, Rev. Mod. Phys. **64**, 755 (1992)
- ⁷ V. G. Karpov, Phys. Rev. B **48**, 12359 (1993).
- ⁸ V. G. Karpov, Phys. Rev. B **48**, 4325 (1993).
- ⁹ V.M. Apalkov, M. E. Raikh, B. Shapiro, Phys. Rev. Lett. **89**, 126601 (2002).
- ¹⁰ V. G. Karpov and E. I. Tsidilkovskii, Phys. Rev. **49**, 4539-4548 (1994).
- ¹¹ V.M. Apalkov, M. E. Raikh, B. Shapiro, Phys. Rev. Lett. **89**, 016802 (2002).
- ¹² V. G. Karpov, JETP Letters, **55** 61 (1992) [Pis'ma Zh. Eksp. Teor. Fiz. **55**, 59 (1992)]
- ¹³ V. G. Karpov and D. W. Oxtoby, Phys. Rev. B **54**, 9734-9745 (1996).
- ¹⁴ A. F. Volkov and Sh. M. Kogan, Soviet Physics, JETP, **25**, 1095 (1967). [J. Exptl. Theoret. Phys. (U.S.S.R.) **52**, 1647 (1967)]
- ¹⁵ V. L. Bonch-Bruevich, I. P. Zvyagin, and A. G. Mironov, *Domain electrical instabilities in semiconductors*, Consultants Bureau, New York (1975).
- ¹⁶ E. Schöll, *Nonlinear Spatio-Temporal Dynamics and Chaos in Semiconductors*, University Press, Cambridge (2001).
- ¹⁷ V.A. Vashchenko and V.F. Sinkevitch, *Physical Limitations of Semiconductor Devices* (Springer, New York, 2008)
- ¹⁸ L. L. Liou, B. Bayraktaroglu, and C. I. Huang, Solid State Electronics, **39**, 165 (1996).
- ¹⁹ Jorgen Olsson, Microelectronic Engineering **56**, 339, (2001)
- ²⁰ G. Breglio, P. Spirito, Microelectronics Journal **31**, 735, (2000)
- ²¹ P. E. Bagnoli and F. Stefani, IEEE Trans. on Components and Packaging Technologies, **32**, 493, (2009)
- ²² O. Semenov, A. Vassighi, and M. Sachdev, IEEE Trans. on Device and Materials Reliability, **6**, 17 (2006)
- ²³ W. S. Tan, P. A. Houston,^a P. J. Parbrook, D. A. Wood, G. Hill, and C. R. Whitehouse, Appl. Phys. Lett., **80** 3207 (2002)
- ²⁴ J. Bolte, F. Niebisch, and J. Pelzl, P. Stelmaszyk and A. D. Wieck, J. Appl. Phys., **84** 15 (1998)
- ²⁵ F. Alagi, Microelectronics Reliability **51**, 321 (2011)
- ²⁶ J.-M. Choi, S.-J. Choi, O. Yarimaga, B. Yoon, J.-M. Kim, and Y.-K. Choi, IEEE Trans. on Electron Devices, **58**, 1570 (2011).
- ²⁷ Xi Wang, Y. Ezzahri, J. Christofferson, and A. Shakouri, J. Phys. D: Appl. Phys. **42**, 075101 (2009)
- ²⁸ E. Pop, K. E. Goodson, J. of Electronic Packaging, **128**, 102 (2006)
- ²⁹ M.-H. Bae, S. Islam, V. E. Dorgan, E. Pop, ACS nano, **5**, 7936, (2011).
- ³⁰ C. Radue and E.E.van Dyk, Solar Energy Materials and SolarCells, **94**, 617622 (2010).
- ³¹ E. L. Meyer, and E. E. van Dyk, Phys. Stat. Sol. (a) **201**, 2245 (2004).
- ³² T. J. McMahon, T. J. Bernard, and D. S. Albin, J. Appl. Phys. **97**, 054503 (2005).
- ³³ J. D. Jackson, Classical Electrodynamics (Wiley, New York,1999).
- ³⁴ D. G. Duffy, *Green's functions with applications*, Chapman and Hall/CRC, New York, London, (2001).
- ³⁵ Diana Shvydka, J. P. Rakotoniaina, and O. Breitenstein, Appl. Phys. Lett., **84**, 729 (2004).
- ³⁶ L. D. Landau and E. M. Lifshitz, *Statistical Physics* 3rd edn (Pergamon, Oxford, 1980).
- ³⁷ D. A. Frank-Kamenetskii, *Diffusion and heat transfer in chemical kinetics*, Second Edition, Plenum Press, New York (1969)
- ³⁸ Ya.B. Zeldovich, G.I. Barenblatt, V.B. Librovich, G.M. Makhviladze, *Mathematical theory of combustion and explosion*. Plenum, New York (1985).
- ³⁹ L. D. Landau and E. M. Lifshitz, *Physics of Fluids*, Second Edition, Pergamon Press, Oxford, New York (1987).
- ⁴⁰ T. Kotoyori, *Critical Temperatures for the Thermal Explosion of Chemicals*, Elsevier, Amsterdam - Boston (2005).
- ⁴¹ P. H. Thomas, Combustion and Flame, **21**, 99 (1973).
- ⁴² A. G. Merzhanov and A. E. Averson, Combustion and Flame, **16**, 89 (1971).
- ⁴³ O. Kallenberg, *Foundations of Modern Probability*, (New York: Springer-Verlag, 1997).
- ⁴⁴ E. M. Lifshitz and L. P. Pitaevskii, *Physical Kinetics* (Elsevier, Amsterdam, Boston, 2008).
- ⁴⁵ D. Kaschiev, *Nucleation: Basic Theory with Applications* Butterworth-Heinemann. Oxford, Amsterdam (2000).
- ⁴⁶ Y. Toyozawa, in *Polarons and Excitons*, edited by C. G. Kuper and G. D. Whitfield (Plenum Press, New York 1962), p. 211.
- ⁴⁷ G. N. Watson, *A treatise on the theory of Bessel functions*, Cambridge 1922.
- ⁴⁸ J. Y. Son and Y.-H. Shina, Appl. Phys. Lett. **92**, 222106 (2008). F. Zhang, X. M. Li, X. D. Gao, L. Wu, X. Cao, X. J. Liu, and R. Yang, J. Appl. Phys. **109**, 104504 (2011). J. J. T. Wagenaar, M. Morales-Masis, and J. M. van Ruitenbeek, J. Appl. Phys. **111**, 014302 (2012).
- ⁴⁹ O. Breitenstein, W. Warta, M. Langenkamp, *Lock-in Thermography: Basics and Use for Evaluating Electronic Devices and Materials*, Springer, 2010.
- ⁵⁰ E. Fermi, *Notes on Quantum Mechanics*, Second Edition, The University of Chicago Press, Chicago (1995).
- ⁵¹ G. A. Korn and T. M. Korn, *Mathematical Handbook for Scientists and Engineers: Definitions, Theorems, and Formulas for Reference and Review* 3d Edition, McGraw Hill (2000).
- ⁵² J. W. Cahn and J. E. Hilliard, J. Chem. Phys., **28**, 258 (1958). *ibid*, **31**, 688 (1960).
- ⁵³ S. M. Sze, *Physics of Semiconductor Devices*, Wiley, New York, 1981.
- ⁵⁴ L. E. Calvet, R. G. Wheeler, and M. A. Reed, Appl. Phys. Lett. **80**, 1761 (2002). R. T. Tung, Phys. Rev. B, **45**, 13509 (1992). V. G. Karpov, M. L. C. Cooray, and Diana Shvydka, Appl. Phys. Lett., **89**, 163518 (2006).
- ⁵⁵ V. N. Smelyanskiy, M. I. Dykman, H. Rabitz, and B. E. Vugmeister, Phys. Rev. Lett., **79**, 3113 (1997).
- ⁵⁶ M. I. Dykman, H. Rabitz, V. N. Smelyanskiy, and B. E. Vugmeister, Phys. Rev. Lett., **79**, 1178 (1997).

⁵⁷ J. S. Langer, *Ann. Phys.* **41**, 108 (1967); S. Coleman, *Phys. Rev. D* **15**, 2929 (1977).